

Collective excitations in liquid and glassy 3-methylpentane

Paola Benassi and Michele Nardone

Dipartimento di Scienze Fisiche e Chimiche, Università degli Studi dell'Aquila, 67100 L'Aquila, Italy

Andrea Giugni

*King Abdullah University of Science and Technology,
PSE and BESE Divisions, Thuwal, 23955-6900, Saudi Arabia*

Giacomo Baldi*

IMEM-CNR, Parco Area delle Scienze 37/A, 43124 Parma, Italy

Aldo Fontana

Dipartimento di Fisica, Università di Trento, 38050 Povo (Trento), Italy

We present a detailed investigation of the terahertz vibrational dynamics of 3-methylpentane performed by means of high resolution inelastic X-ray scattering (IXS). We probe the dynamics in a large temperature range, which includes the glass, the supercooled liquid and the liquid phases. The characteristic frequency of the excitations follows a well defined dispersion curve extending beyond 8 nm^{-1} at all the investigated temperatures, indicating the persistence of a solid-like behaviour also in the liquid phase. This implies the existence of a pseudo-Brillouin zone whose size compares surprisingly well with the periodicity inferred from the first sharp diffraction peak in the static structure factor. We show that, in the investigated temperature range, both sizes undergo a variation of about 15-20 %, comparable to that of the average intermolecular distance. We finally show that the IXS sound velocity coincides with the infinite frequency sound velocity previously inferred from visible and ultraviolet Brillouin spectroscopy data. This analysis confirms the role of the shear relaxation processes in determining the variation with frequency of the apparent sound velocity.

PACS numbers: 63.50.Lm, 64.70.kj, 61.05.C-, 61.43.Fs

I. INTRODUCTION

The existence of propagating collective excitations at large exchanged wavevector values in systems which do not possess translational order, such as amorphous solids and liquids, has been widely demonstrated by inelastic X-ray scattering¹⁻⁵ and by neutron scattering experiments⁶⁻⁹. These excitations exhibit a dispersion relation which closely resembles that of longitudinal modes of a crystalline solid, extending in some cases even beyond what we can refer to as a pseudo-Brillouin zone. The boundary of this pseudo-Brillouin zone generally occurs at wavevectors roughly one half of the first maximum, q_m , of the static structure factor $S(q)$ ¹⁰.

In this paper we report measurements of IXS spectra of 3-methylpentane (3MP) at different exchanged wavevectors q extending up to q_m and covering the temperature range from room temperature down to the glass transition. Such measurements will be analyzed in order to characterize the behavior of the collective excitations and their relationship with the propagation of sound in this glass-forming liquid.

3MP is a structural isomer of hexane, molecular formula C_6H_{14} , formed by a pentane chain with a methyl group bonded to the third carbon atom. It belongs to a group of molecules referred to as branched-chain alkanes¹¹ or as methylated alkanes¹². It is a non polymeric glass-forming liquid with a calorimetric glass transition temperature at $T_G \approx 77 \text{ K}$ ¹³⁻¹⁵. The glassy phase is read-

ily formed by cooling the liquid below the glass transition temperature, thus allowing us to study the behavior of both liquid and disordered solid phases. Because of the relatively small atomic number Z , it can be successfully measured in an IXS experiment.

It will be shown that the analysis of the spectra yields dispersion curves which are well defined also above the pseudo-Brillouin zone boundary, not only in the glassy phase but also in the liquid up to room temperature. These dispersion curves exhibit maxima which are found to fall close to $q_m/2$ (as obtained from measurements of the structure factor $S(q)$) at all temperatures, yielding a pseudo lattice parameter a_0 which increases monotonically with temperature.

The apparent sound velocity, as obtained from the initial slope of these curves, favorably compares with the high frequency sound velocities inferred from visible and ultraviolet Brillouin spectroscopy¹⁶. This comparison confirms the role of shear relaxation processes in determining the difference between zero frequency and infinite frequency sound velocities in this system.

II. EXPERIMENTAL DETAILS AND DATA ANALYSIS

The sample (3MP > 99% purity) supplied by Sigma Aldrich, was contained in an aluminium vessel equipped with high transmittance Kapton windows which con-

tribute negligibly to the collected scattered intensity.

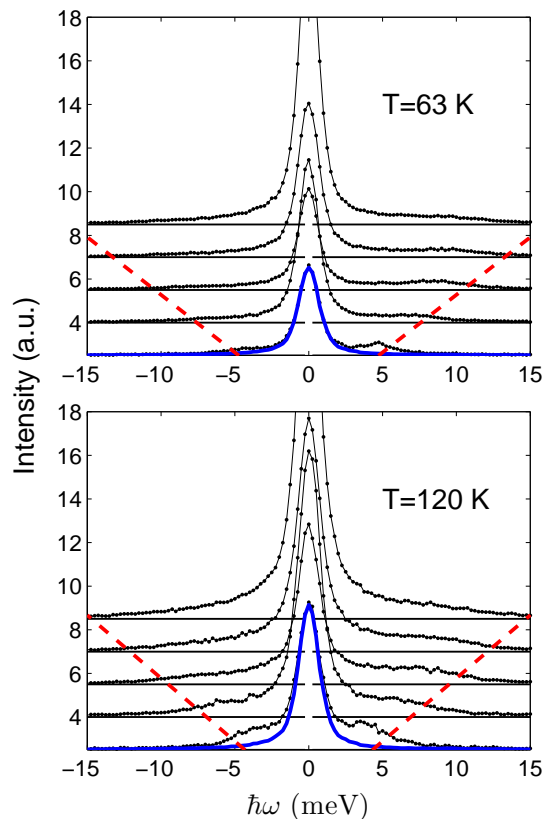


FIG. 1. (Color online). Selection of IXS spectra (black dots) as measured at $T = 120$ K in the liquid phase (bottom panel) and at $T = 63$ K in the glassy phase (top panel). The spectra are vertically shifted by an amount proportional to the exchanged wavevector (from bottom to top, $q = 2, 5, 4.0, 5.5, 7.0$ and 8.5 nm^{-1}). The full line (blue) is the measured instrumental transfer function while the dashed line (red) is the linear dispersion obtained using the apparent sound velocity (see discussion).

The spectral measurements were performed at the high energy resolution beam-line ID16 of the European Synchrotron Radiation Facility in Grenoble, France. The X-ray beam (incident energy $E_0 = 21747$ eV) impinges on the sample and the scattered radiation is analyzed by means of a 6.5 m long arm hosting the crystal analyzers. The exchanged wave vector q is selected by rotating the analyzer arm. Energy scans are performed at constant momentum transfer (between 1 and 14.5 nm^{-1} in our case) by varying the relative temperatures of the monochromator crystal with respect to the analyzer crystals. Further details on the beam-line are reported elsewhere¹⁷. We measured the overall spectrometer transfer function at each analyzer by measuring the elastic scattering from a PMMA sample. The PMMA was cooled at $T = 10$ K and measured at the exchanged

wavevector q corresponding to the maximum of its structure factor where the inelastic scattering contribution to the spectrum is negligible. The resolution profile $R(\omega)$ of all the analyzers turns out to be essentially Lorentzian with a FWHM of about 1.5 meV.

Figure 1 shows, as an example, the IXS experimental data for $T = 120$ K in the liquid phase and for $T = 63$ K in the glassy phase at different qs together with a typical instrumental resolution profile. Each spectrum is obtained by averaging four energy scans, lasting typically 45 minutes, after normalization to the intensity of the incident beam.

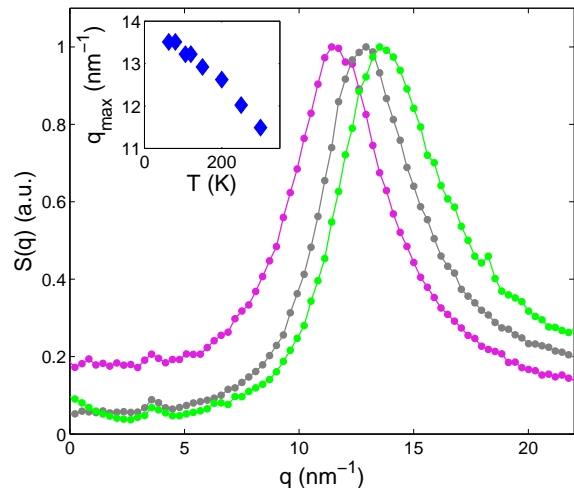


FIG. 2. (Color online). Measured static structure factor $S(q)$ at selected temperatures (from left to right): $T = 300$ K (magenta), $T = 150$ K (grey) and $T = 63$ K (green). The intensities of the data are arbitrarily normalized to their maxima. The inset shows the temperature behavior of the position q_{max} of the first sharp diffraction peak. These values have been obtained fitting $S(q)$ with a parabola around its maximum.

The total scattered intensity, $S(q)$, has also been measured at all temperatures as a function of q . Selected $S(q)$ are reported in figure 2 with intensities normalized to their maxima. The shift in the position, q_{max} , of the first sharp diffraction peak is evident at increasing temperature.

At small wavevectors the spectra show, at all temperatures, evidence of well defined side peaks which exhibit detailed balance between Stokes and anti-Stokes sides. These side peaks become broader and less prominent as q is increased and are hardly detectable above 10 nm^{-1} , particularly in the liquid phase. All the spectra exhibit a relatively intense central line with a linewidth comparable with that of the resolution profile, even though some broadening can be detected at the highest q values and high temperature.

On the basis of these evidences we have analyzed these spectra using a normalized simple damped harmonic os-

cillator lineshape (DHO), assuming:

$$I(\omega) \propto R(\omega) \otimes [A \cdot \delta(\omega) + S_{DHO}(q, \omega)] + B,$$

where

$$S_{DHO}(q, \omega) = f(\omega, T) \frac{1}{\pi} \frac{\omega_0^2(q) \Gamma(q)}{[\omega^2 - \omega_0^2(q)]^2 + \omega^2 \Gamma^2(q)}$$

and

$$f(\omega, T) = \frac{\hbar\omega}{KT} \left[\frac{1}{1 - \exp(-\frac{\hbar\omega}{KT})} \right]$$

accounts for detailed balance. The physically relevant free fit parameters are the frequency ω_0 , the damping Γ and the amplitude A of the elastic contribution relative to the inelastic one. B accounts for a small background of the order of a few counts for each spectrum.

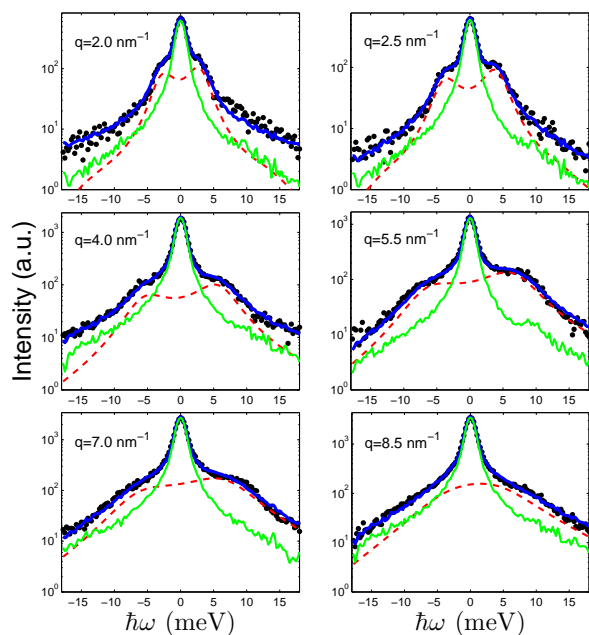


FIG. 3. (Color online). IXS spectra (black dots) measured at $T = 120$ K for selected values of q . The logarithmic intensity scale allows one to appreciate the details of the instrumental transfer function (thin green solid line) and of the inelastic contribution of the fitting function (red dashed line). The reconstructed profile $I(\omega)$ is shown as a thick solid line (blue).

Some typical fits are shown in figure 3 for $T = 120$ K and for $2 \leq q \leq 8.5$ nm^{-1} . The quality of the fits is comparably good at all other temperatures, the χ^2 values being always of the order of unity. At high q values, however, the simple lineshape adopted appears to become progressively less adequate in describing the spectra. In particular, for the highest q values and at high temperatures, the side peaks intensity decreases considerably and the central line slightly broadens. As a consequence, the relative intensity of the two spectral contributions becomes unreliable.

III. RESULTS AND DISCUSSION

In this paper we focus our attention mainly on the temperature and wavevector behavior of the parameter ω_0 . The values of ω_0 , as obtained from the fitting of the spectral lineshapes, are reported in figure 4 as a function of q for different temperatures. The values of ω_0 exhibit a well defined linear dispersion at low q s typical of the hydrodynamic behavior. More interestingly, at larger q s the dispersion relation presents a maximum, located in the range $6 - 8$ nm^{-1} , which is well defined at all temperatures in both liquid and solid phases.

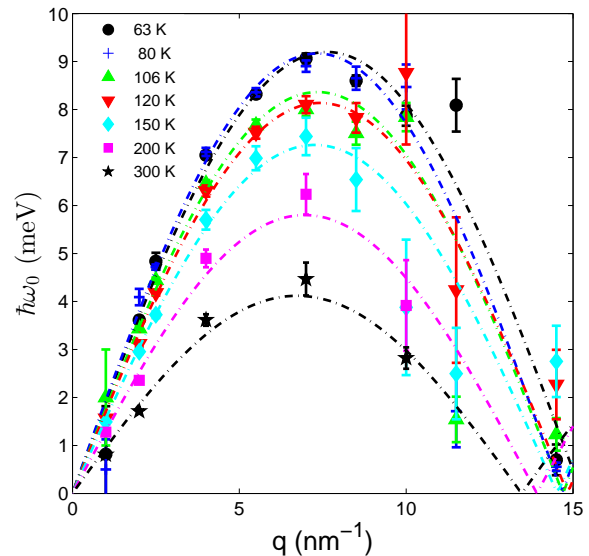


FIG. 4. (Color online). The fitting parameter ω_0 versus q (see text) at different temperatures as indicated in the legend. For each temperature the line is the best fit of equation 1 to the data. The high q data, typically above 8.5 nm^{-1} have not been included in the fitting procedure.

We have parametrized this behavior using a simple sinusoidal dispersion of the form¹⁸:

$$E = \hbar\omega = \hbar v \frac{2q_0}{\pi} \left| \sin \left(\frac{\pi q}{2q_0} \right) \right| \quad (1)$$

which is characterized by an initial slope, determining the apparent sound velocity v , being $E \simeq \hbar v q$, and by the occurrence of a maximum for $q = q_0$. The q_0 values can be related to the pseudo-Brillouin zone boundary wavevector characterized by a "lattice parameter" $a_0 = \pi/q_0$ describing the local range order. The parameters v and q_0 have been determined fitting the data excluding those at the higher wavevector and temperatures, where the spectral fitting procedure appeared, as already mentioned, to be less reliable. Looking at figure 4 it should be noted that this very simple model describes surprisingly well the experimental results.

The values of the apparent sound velocity v are shown, as a function of temperature, in figure 5, together with

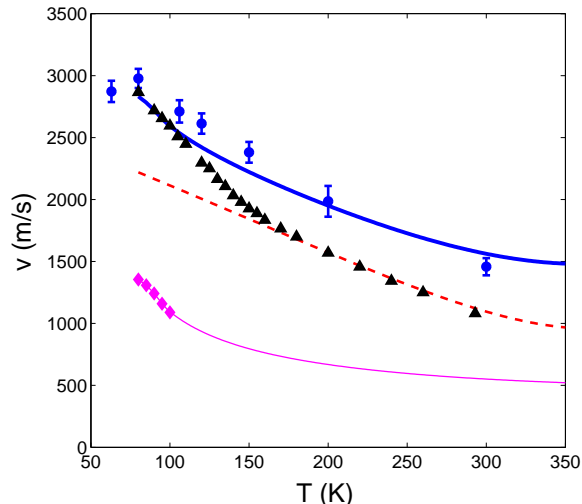


FIG. 5. (Color online). Apparent sound velocity v versus temperature as obtained from IXS measurements (blue dots) and from Brillouin scattering measurements at 90° with 266 nm excitation (black triangles). The full thick line (blue) and the dashed line (red) represent respectively the infinite and zero frequency limits, as argued from¹⁶. Diamonds are the transverse velocities measured by Brillouin scattering at 90° with 532 nm excitation together with the extrapolation of their high temperature behavior (thin solid line, magenta) following Barlow²⁰.

those obtained from 90° Brillouin scattering spectra measured with 266 nm excitation¹⁶, corresponding to exchanged wavevectors of about 0.05 nm^{-1} .

In figure 6 we report the values of the pseudo lattice parameter a_0 as a function of temperature together with the corresponding values obtained from the first diffraction maximum q_{max} , i.e.:

$$a_m = \frac{2\pi}{q_{\text{max}}}$$

Both a_m and a_0 , which are numerically quite similar, exhibit a weak temperature dependence (see figure 6) which well compares with that of the average intermolecular distance given by:

$$a = \left(\frac{1}{\rho}\right)^{\frac{1}{3}}$$

ρ being the molecular number density obtained from reference¹⁹. The values of $a_m(T)$ appear to be systematically larger than those of $a_0(T)$. This could be due to the presence of the intramolecular interference term which has not been taken into account in analyzing diffraction data.

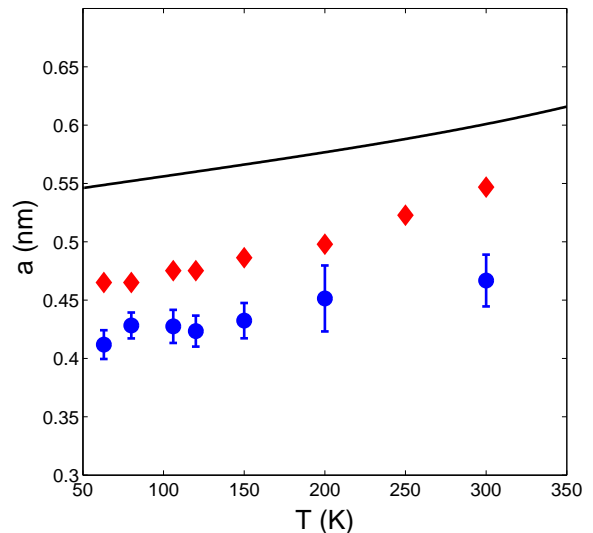


FIG. 6. (Color online). Characteristic length a versus temperature. The a_0 values (blue full dots) are obtained fitting the dispersion curves (see text) while a_m values (red diamonds) are obtained from the maxima of $S(q)$. The full (black) line is obtained from density data (see text).

IV. CONCLUSIONS

The inelastic X-ray scattering spectra from liquid and amorphous solid *3MP* reported in this work show propagating collective excitations that are well defined in a rather wide temperature range, extending from room temperature down to the glass transition temperature, and for exchanged wavevector values as large as those of the first sharp diffraction peak. Analyzing the spectra in terms of a simple DHO lineshape we have derived dispersion curves from which we have obtained the temperature dependence of the apparent sound velocity $v(T)$ and of the pseudo lattice parameter $a_0(T)$.

The values of $a_0(T)$, which have been obtained analyzing dynamic properties of the system are compared with those of $a_m(T)$ derived from purely structural properties. The comparison shows that both quantities increase almost linearly with temperature, following essentially the behavior of the average intermolecular distance a , and yielding a variation of about 15%-20%, in the entire investigated range. The smooth behavior of both quantities across the glass transition confirms that no severe structural changes occur in this molecular liquid upon vitrification.

The apparent sound velocity is compared in figure 5 with sound velocity values reported in a recent paper¹⁶. In that paper some of us performed a thorough analysis of both longitudinal and transverse relaxation processes in fluid *3MP* analyzing Brillouin spectra at different scattering angles and different excitation wavelengths (532 nm and 266 nm). It was found that, on the basis of the observed transverse modes velocity (diamonds in fig-

ure 5), both longitudinal and shear viscosity relaxation processes are required in order to justify the observed linewidths of the longitudinal Brillouin peaks. The identification and characterization of both these processes allowed the authors to obtain the "infinite frequency" sound velocity (full line in the same figure). The apparent sound velocity determined by the longitudinal Brillouin peak position (up triangles in the figure) is seen to coincide with the "infinite frequency" values at temperatures close to T_G , while, as the temperature is increased, it tends to the "zero frequency" limit (dash-dotted line) given by ultrasonic measurements. The IXS data of the present work are indeed in very good agreement with

these "infinite frequency" values, confirming the validity of the previous analysis.

V. ACKNOWLEDGMENTS

We gratefully acknowledge the prolific debates and stimulating discussions with the late Professor Marco Sampoli who has brought to our attention the interesting phenomenology of this glass forming liquid. We are grateful to Francesco Albergamo at ESRF for providing assistance in using beamline ID16. We acknowledge Silvia Caponi for the useful discussions.

* giacomo.baldi@cnr.it

- ¹ T. Scopigno, G. Ruocco, and F. Sette, *Rev. Mod. Phys.* **77**, 881 (2005).
- ² A. Matic, C. Masciovecchio, D. Engberg, G. Monaco, L. Börjesson, S. C. Santucci, and R. Verbeni, *Phys. Rev. Lett.* **93**, 145502 (2004).
- ³ V. V. Brazkin and K. Trachenko, *J. Phys. Chem. B* **118**, 11417 (2014).
- ⁴ B. Ruzicka, T. Scopigno, S. Caponi, A. Fontana, O. Pilla, P. Giura, G. Monaco, E. Pontecorvo, G. Ruocco, and F. Sette, *Phys. Rev. B* **69**, 100201 (2004).
- ⁵ G. Baldi, M. Zanatta, E. Gilioli, V. Milman, K. Refson, B. Wehinger, B. Winkler, A. Fontana, and G. Monaco, *Phys. Rev. Lett.* **110**, 185503 (2013).
- ⁶ L. E. Bove, E. Fabiani, A. Fontana, F. Paoletti, C. Petrillo, O. Pilla, and I. C. V. Bento, *Europhys. Lett.* **71**, 563 (2005).
- ⁷ E. Fabiani, A. Fontana, and U. Buchenau, *J. Chem. Phys.* **128**, 244507 (2008).
- ⁸ L. Orsingher, G. Baldi, A. Fontana, L. E. Bove, T. Unruh, A. Orecchini, C. Petrillo, N. Violini, and F. Sacchetti, *Phys. Rev. B* **82**, 115201 (2010).
- ⁹ M. Zanatta, A. Fontana, A. Orecchini, C. Petrillo, F. Sacchetti, *J. Phys. Chem. Lett.* **4** 1143 (2013).
- ¹⁰ U. Balucani and M. Zoppi, *Dynamics of the liquid state* (Clarendon Press, Oxford, 1994).
- ¹¹ S. Shahriari, A. Mandanici, L.-M. Wang, and R. Richter, *J. Chem. Phys.* **121**, 8960 (2004).
- ¹² K. L. Ngai, *Phys. Rev. B* **71**, 214201 (2005).
- ¹³ A. C. Ling and J. E. Willard, *J. Phys. Chem.* **72**, 1918 (1968).
- ¹⁴ H. L. Finke and J. F. Messerly, *J. Chem. Thermodyn.* **5**, 247 (1973).
- ¹⁵ L. M. Wang, C. A. Angel, and R. Richert, *J. Chem. Phys.* **125**, 074505 (2006).
- ¹⁶ P. Benassi, M. Nardone, and A. Giugni, *J. Chem. Phys.* **137**, 094504 (2012).
- ¹⁷ C. Masciovecchio, U. Bergmann, M. H. Krisch, G. Ruocco, F. Sette, and R. Verbeni, *Nucl. Instrum. Methods* **111**, 181 (1996).
- ¹⁸ C. Kittel, *Introduction to Solid State Physics* (John Wiley and Sons, New York, 1966).
- ¹⁹ A. A. Ruth, B. Nickel, and H. Lesche, *Z. Phys. Chem.* **175**, 91 (1992).
- ²⁰ J. Barlow and J. Lamb, *Discuss. Faraday Soc.* **43**, 223 (1967).